Preprints, 4th IFAC Conference on
Advances in Proportional-Integral-Derivative Control
Almería, Spain | June 12-14, 2024

SIR Epidemic Control Using a 2DoF IMC-PID with Filter Control Strategy

D. E. Rivera [*,⋆] S. Banerjee [*] C. Kobs [*] M. El Mistiri [*] Z. Shi [*]

[*] *Control Systems Engineering Laboratory, School for Engineering of Matter, Transport, and Energy, Ira A. Fulton Schools of Engineering, Arizona State University, Tempe, AZ, USA*

Abstract: The COVID-19 pandemic has given rise to many significant research activities, among these a resurgence of the use of control-oriented approaches for modeling and controlling epidemics. An examination of a SIR (Susceptible-Infectious-Recovered) dynamic model under endemic conditions using Internal Model Control (IMC) shows that a two-degree-of-freedom (2DoF) PID with filter structure is a natural solution for understanding how to manage a pandemic, with model-based IMC-PID tuning being extremely effective when evaluated on a first-principles, nonlinear plant model. Dynamic modeling (nonlinear and linearized), PID controller design, and closed-loop evaluation (under conditions that include vaccination and the loss of immunity/potential for re-infection) are presented, with the results demonstrating the deep insights that can be gained from simple models and control policies. Computational models as presented in this work could be used to inform the actions of governments and individuals.

Keywords: Process control applications, epidemic modeling and control, model-based PID controller tuning.

1. INTRODUCTION

The COVID-19 pandemic is a significant world event that remains among us, and has touched every individual on the planet in some way. It is difficult to find someone whose family or loved ones have been unaffected or not impacted. The pandemic nonetheless has brought about unexpected opportunities for education and research, which include contributions to the field of process control (in general) and PID controller tuning (in particular).

This work is based on experiences using an epidemic model, namely, a Susceptible-Infectious-Recovered (SIR) model, to teach process dynamics and control to chemical engineering undergraduates taking CHE 461: Process Dynamics and Control, a required course in the chemical engineering curriculum at Arizona State University. Our initial efforts were documented in a paper presented at the 13th IFAC Workshop on Advances in Control Education (ACE 2022; Rivera et al. (2022)). While that paper focused on educational outcomes and how the problem was integrated in ChE 461, this paper takes a more expansive look, providing a broader, more comprehensive problem statement (that includes vaccination and loss of immunity); important details (such as the derivation of the model-based IMC-PID tuning rules) are also explained.

The paper is organized as follows. Section 2 describes an open-loop dynamical model and linearization, Section 3 describes the IMC-PID controller design, Section 4 shows some simulations, and Section 5 describes future work. We conclude with a description of extensions and current and future efforts on the problem.

[⋆] To whom all correspondence should be addressed (e-mail: daniel.rivera@asu.edu).

2. SIR MODEL FOR DISEASE TRANSMISSION

Compartmental models used in epidemiology to model infectious disease can be understood using a chemical reactor analogy, where disease transmission and remission correspond to an autocatalytic reaction with catalyst deactivation (Simon, 2020). In particular, we are interested in developing a dynamical model for a variation of the classical Susceptible-Infectious-Recovered (SIR) problem (Kermack and McKendrick, 1927) that considers births, deaths, and time-varying transmission $\beta(t)$ and recovery $\gamma(t)$ rates. A problem schematic is shown in Figure 1, illustrating the problem in terms of a continuously-stirred tank reactor (Levenspiel, 1998).

The goal of the model is to determine how the populations of Susceptible ($S(t)$), Infectious ($I(t)$), and Recovered/Removed ($R(t)$)) individuals, as well as the rates of infection, deactivation, vaccination, and loss of immunity change over time during an epidemic. For simplicity, the inflow to the reactor B_r (the number of births/day) is considered constant, as well as mortality rates per day for each of the populations ($\mu = \mu_S = \mu_I = \mu_R$, respectively). Correspondingly, the total population $N = S(t) + I(t) + R(t)$ remains constant, with the population of Removed individuals $R(t)$ computed from the solutions to $S(t)$ and $I(t)$. The incidence rate, i.e., the number of new infections per day, is determined by the autocatalytic reaction with constitutive expression,

$$S + I \overset{\beta(t)}{\rightarrow} 2I \qquad r_{infect} = \beta(t)S(t)I(t) \tag{1}$$

The time-varying transmission rate $\beta(t)$ is influenced by government mandates for social distancing and hygienic procedures (e.g., mask-wearing). Hence, it is a variable that could be considered to be "adjustable" by society and

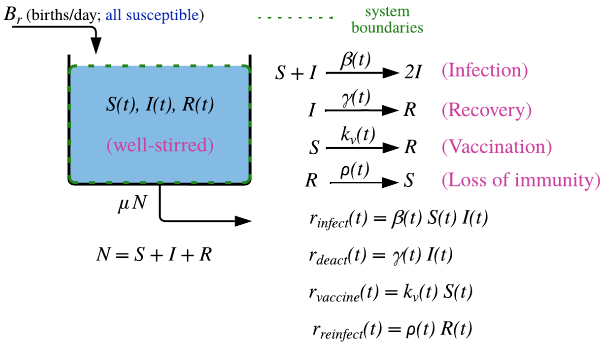

Fig. 1. SIR disease modeling as a continuously-stirred tank reactor (CSTR) featuring autocatalytic (infection) and deactivation (recovery) reactions, as well as the effects of vaccination and loss of immunity.

thus falls as manipulated. A lower value for β results in a decrease in the infection rate, and would result in a decrease in the number of infected individuals. Recovery (i.e., deactivation) of infected individuals per day is described by a first-order reaction

$$I \overset{\gamma(t)}{\to} R \qquad r_{deact} = \gamma(t)I(t) \tag{2}$$

The recovery rate $\gamma(t)$ is time-varying, with γ^{-1} corresponding to the average duration of infectiousness. Increasing γ implies that infected individuals remain infectious for a shorter amount of time, which would ultimately result in a decrease in the infected population. Actions such as the availability of more effective treatments and therapeutics can influence γ. In this work, we will consider $\gamma(t)$ as an exogenous variable that is external to the process and can thus be treated as a disturbance.

A natural consideration in this problem is to examine the influence of vaccination rates. The effect of vaccines is to take susceptible individuals directly to the removed category. Vaccination of susceptible individuals per day can be described by a first-order reaction

$$S \overset{k_v(t)}{\to} R \qquad r_{vacc} = k_v(t)S(t) \tag{3}$$

with the rate of vaccination $k_v(t)$ now serving as an additional disturbance to the problem. Incorporating this problem feature in the nonlinear model and step testing this additional disturbance (from $k_v = 0$ to some value) will have a significant positive influence on the problem.

Finally, an important aspect of the problem that has been an unavoidable reality in the current pandemic is the possibility of loss of immunity, where recovered individuals can return to the susceptible population, and hence are candidates for possible re-infection. Loss of immunity can be described as a first-order reaction according to:

$$R \overset{\rho(t)}{\to} S \qquad r_{reinfect} = \rho(t)R(t) \tag{4}$$

As with $\gamma(t)$ and $k_v(t)$, we consider that the loss of immunity parameter $\rho(t)$ is also an exogenous influence to the problem (and acts as a disturbance to the problem).

With this information in hand, it becomes possible to write species accounting equations that describe the dynamics of this system; these equations can then be expressed as a nonlinear lumped parameter model amenable to integration in computational tools such as MATLAB w/Simulink:

$$\frac{dx}{dt} = f(x,u,d) \tag{5}$$

$$y = g(x,u,d) \tag{6}$$

The nonlinear lumped parameter system consistent with the problem statement can be obtained from (7)-(11):

$$\begin{aligned}\frac{dS(t)}{dt} = \underbrace{B_r}_{\substack{Births\\(inflow)}} - \underbrace{\beta(t)S(t)I(t)}_{\substack{Infection\\(consumption)}} - \underbrace{\mu S(t)}_{\substack{Mortality\\(outflow)}} = f_1(x,u,d)\\ - \underbrace{k_v(t)S(t)}_{\substack{Vaccination\\(consumption)}} + \underbrace{\rho(t)\left(\frac{B_r}{\mu} - S(t) - I(t)\right)}_{\substack{Loss\ of\ Immunity/Reinfection\\(generation)}}\end{aligned} \tag{7}$$

$$\frac{dI(t)}{dt} = \underbrace{\beta(t)S(t)I(t)}_{\substack{Infection\\(consumption)}} - \underbrace{\gamma(t)I(t)}_{\substack{Deactivation\\(consumption)}} - \underbrace{\mu I(t)}_{\substack{Mortality\\(outflow)}} = f_2(x,u,d) \tag{8}$$

$$x = \begin{bmatrix} S(t) \\ I(t) \end{bmatrix}, \qquad u = [\beta(t)], \qquad d = \begin{bmatrix} \gamma(t) \\ k_v(t) \\ \rho(t) \end{bmatrix} \tag{9}$$

$$f(x,u,d) = \begin{bmatrix} f_1 \\ f_2 \end{bmatrix}, \qquad y = \begin{bmatrix} S(t) \\ I(t) \\ R(t) \\ r_{infect}(t) \end{bmatrix} \tag{10}$$

$$g(x,u,d) = \begin{bmatrix} g_1 \\ g_2 \\ g_3 \\ g_4 \end{bmatrix} = \begin{bmatrix} S(t) \\ I(t) \\ \dfrac{B_r}{\mu} - S(t) - I(t) \\ \beta(t)S(t)I(t) \end{bmatrix} \tag{11}$$

Linearization leads to a model in state-space form,

$$\begin{aligned}\frac{d\Delta x}{dt} &= A\ \Delta x + B\ \Delta u + \Gamma\ \Delta d \\ \Delta y &= C\ \Delta x + D_u\ \Delta u + D_d\ \Delta d\end{aligned} \tag{12}$$

where A, B, Γ, C, D_u and D_d are constant-valued matrices, while Δ denotes deviation variables. $\bar{x}$, $\bar{u}$, $\bar{d}$, and $\bar{y}$ represent initial steady-state conditions obtained by solving $f(\bar{x},\ \bar{u},\ \bar{d}) = 0$. For the problem at hand there are two steady-state conditions, with the most interesting case (denoting endemic conditions) consisting of (shown here for $\bar{k}_v = 0$):

$$\bar{S} = \frac{(\mu + \bar{\gamma})}{\bar{\beta}} \tag{13}$$

$$\bar{I} = -\frac{(\bar{\gamma}\mu^2 + \bar{\rho}\mu^2 + \mu^3 - B_r\bar{\beta}\mu - B_r\bar{\beta}\bar{\rho} + \bar{\gamma}\mu\bar{\rho})}{\bar{\beta}(\bar{\gamma}\mu + \bar{\rho}\mu + \mu^2)} \tag{14}$$

$$\bar{R} = \frac{B_r}{\mu} - \bar{S} - \bar{I} \tag{15}$$

The steady-state according to (13)-(15) results in $\bar{I} \neq 0$ from which an informative linearized model useful for control design can be obtained.

An effective computational model (such as one from MATLAB and Simulink) can be used to generate representative step responses for *independent* changes in *each* input variable (β, γ, k_v, and ρ) for the base parameters ($B_r = 500$, $\mu = 0.1$). For each input, it is possible to produce a *non-trivial* change that shows when the linear model is a valid approximation for this system and a second change that highlights process nonlinearity. To illustrate some desired simulation results, a set of model responses (linear and nonlinear) to a β change of -0.0004 (at time $t = 10$ days), a γ change of +0.4 (at time $t = 40$ days), a k_v change of +0.2 (at time t=80 days), and a ρ change of +0.25 (at time $t = 120$ days) for parameters $B_r = 500$, $\mu = 0.1$, $\bar{\beta} = 0.0008$, $\bar{\gamma} = 0.25$, $\bar{k}_v = 0$, and $\bar{\rho} = 0.1$ are shown in Figure 2. A symbolic transfer function for all problem inputs (from MATLAB's `Symbolic Math Toolbox`) is shown in Figure 3, with the numerical transfer function generated by MATLAB (in gain-time constant form) (for β changes only) shown in Figure 4, The following observations ensue:

(1) All model responses agree with physical intuition, i.e., increasing β increases the infected population while increasing Γ reduces it.
(2) The linearized and nonlinear model responses agree qualitatively (e.g., shape, speed, and direction) but can differ quite substantially in magnitude.
(3) Despite this, the linearized transfer function expressions are useful in predicting the *intrinsic* dynamic behavior of this system.

The linearized plant model (both numerical and symbolic) includes the following insights:

- The plant response characteristics can range from underdamped to overdamped, based on operating conditions.
- The nominal linearized transfer function model describing the dynamics between $\beta(t)$ and $I(t)$ conforms to a second-order transfer function according to:
$$\tilde{p}(s) = \frac{b_1 s + b_2}{s^2 + a_1 s + a_2} \qquad (16)$$
- The symbolic transfer function model from Fig. 3 shows that, *over all operating conditions*, 1) the steady-state gain for (16) is always greater than zero, which implies that lowering β will always reduce the infected population, and 2) the plant zero in the transfer function (16) will always lie in the Left-Half Plane (LHP). This latter characteristic greatly simplifies the application of the IMC design procedure to obtain a feedback control law, as the IMC controller $\tilde{q} = \tilde{p}^{-1}$ will always be stable and causal, requiring only a first-order filter to be made semiproper.

On the basis of this modeling effort and insights gained from open-loop responses and transfer functions, it becomes possible to examine PID controller design for this problem, as explained in the ensuing section.

3. PID CONTROLLER DESIGN

The control strategy to be evaluated relies on the transmission rate constant $\beta(t)$ as a manipulated variable ($u(t)$) to reduce the infected population $I(t)$ (the controlled variable $y(t)$) to a desired setpoint, all while in the presence of "disturbances" arising from changes in the rate constants $\gamma(t)$, $k_v(t)$, and $\rho(t)$. Design requirements for the control system are as follows:

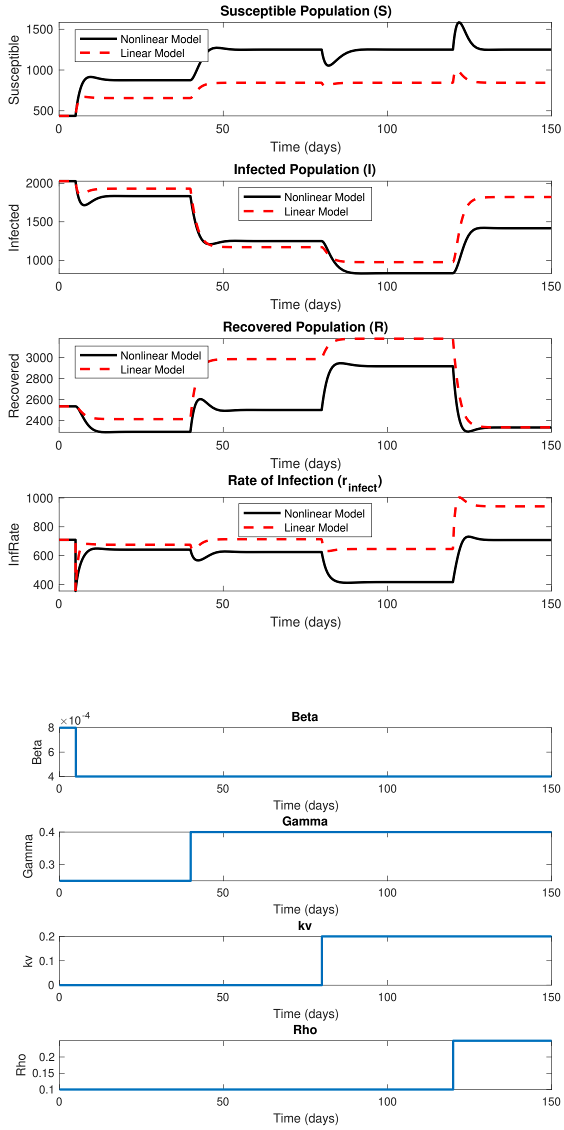

Fig. 2. Susceptible, infected, removed population responses and infection rate for linear and nonlinear models to a β change of -0.0004 (occurring at time $t = 10$ days), a γ change of +0.15 (occurring at time $t = 40$ days), a k_v change of +0.2 (occurring at time $t = 80$ days), and a ρ change of +0.15 (occurring at time $t = 120$ days) for parameters $B_r = 500$, $\mu = 0.1$, $\bar{\beta} = 0.0008$, $\bar{\gamma} = 0.25$, $\bar{k}_v = 0$, and $\bar{\rho} = 0.1$.

(1) The control system must not differentiate step setpoint changes;
(2) Controlled variable responses should be smooth with little or no oscillation; preferably no more than 10% overshoot (or undershoot) for a step setpoint change,
(3) The closed-loop speed of response should be comparable (and preferably faster) than the open-loop speed of response,
(4) While an abrupt change may initially be necessary in the manipulated variable response, the controller should avoid taking $\beta(t)$ to 0 (i.e., full lockdown)

$$\begin{pmatrix} -\frac{\mathrm{Infec\,Suscpt}\,(\gamma+\mu+\rho+s)}{\sigma_1} & \frac{\mathrm{Infec}\,(\rho+\mathrm{Suscpt}\,\beta)}{\sigma_1} & -\frac{\mathrm{Suscpt}\,\sigma_4}{\sigma_1} & -\frac{\sigma_5\,\sigma_4}{\sigma_1} \\ \frac{\mathrm{Infec\,Suscpt}\,(\mathrm{kv}+\mu+\rho+s)}{\sigma_1} & -\frac{\mathrm{Infec}\,(\mathrm{kv}+\mu+\rho+s+\mathrm{Infec}\,\beta)}{\sigma_1} & -\frac{\mathrm{Infec\,Suscpt}\,\beta}{\sigma_1} & -\frac{\mathrm{Infec}\,\beta\,\sigma_5}{\sigma_1} \\ \frac{\mathrm{Infec\,Suscpt}\,(\gamma-\mathrm{kv})}{\sigma_1} & \frac{\mathrm{Infec}\,(\mathrm{kv}+\mu+s+\mathrm{Infec}\,\beta-\mathrm{Suscpt}\,\beta)}{\sigma_1} & \frac{\mathrm{Suscpt}\,\sigma_2}{\sigma_1} & \frac{\sigma_3\,\sigma_2}{\mu\,\sigma_1} \\ \frac{\mathrm{Infec\,Suscpt}\,(\gamma+\mu+s)\,(\mathrm{kv}+\mu+\rho+s)}{\sigma_1} & -\frac{\mathrm{Infec}\,\beta\,(\mathrm{Suscpt\,kv}-\mathrm{Infec}\,\rho+\mathrm{Suscpt}\,\mu+\mathrm{Suscpt}\,\rho+\mathrm{Suscpt}\,s)}{\sigma_1} & -\frac{\mathrm{Infec\,Suscpt}\,\beta\,(\gamma+\mu+s)}{\sigma_1} & -\frac{\mathrm{Infec}\,\beta\,\sigma_3\,(\gamma+\mu+s)}{\mu\,\sigma_1} \end{pmatrix}$$

where

$$\sigma_1 = \gamma\,\mathrm{kv} + \gamma\,\mu + \mathrm{kv}\,\mu + \gamma\,\rho + \gamma\,s + \mathrm{kv}\,s + \mu\,\rho + 2\,\mu\,s + \rho\,s + \mu^2 + s^2 + \mathrm{Infec}\,\beta\,\gamma + \mathrm{Infec}\,\beta\,\mu + \mathrm{Infec}\,\beta\,\rho + \mathrm{Infec}\,\beta\,s - \mathrm{Suscpt}\,\beta\,\mathrm{kv} - \mathrm{Suscpt}\,\beta\,\mu - \mathrm{Suscpt}\,\beta\,\rho - \mathrm{Suscpt}\,\beta\,s$$

$$\sigma_2 = \gamma + \mu + s + \mathrm{Infec}\,\beta - \mathrm{Suscpt}\,\beta$$

$$\sigma_3 = \mathrm{Infec}\,\mu - \mathrm{Brate} + \mathrm{Suscpt}\,\mu$$

$$\sigma_4 = \gamma + \mu + s - \mathrm{Suscpt}\,\beta$$

$$\sigma_5 = \mathrm{Infec} + \mathrm{Suscpt} - \frac{\mathrm{Brate}}{\mu}$$

Fig. 3. Symbolic transfer functions for the linearized model, obtained from the `Symbolic Math Toolbox` in MATLAB. The absence of RHP zeros in the (2,1) element (i.e., the transfer function between $\Delta\beta(s)$ and $\Delta I(s)$) over all practical operating conditions simplifies the use of IMC, and has a significant impact on control design.

```
From input "Beta" to output...
                  -5.4687e05 (1+2.222s)
  Susceptible:  ----------------------
                (1+0.8146s) (1+1.682s)

                2.4306e05 (1+5s)
  Infected:  ----------------------
             (1+0.8146s) (1+1.682s)

                   3.0382e+05
  Recovered:  ----------------------
              (1+0.8146s) (1+1.682s)

                  85069 (1+2.857s) (1+5s)
  InfectedRate:  ----------------------
                 (1+0.8146s) (1+1.682s)
```

Fig. 4. MATLAB-generated numerical transfer functions in gain-time constant form (for β changes only) resulting from steady-state conditions obtained from parameters $B_r = 500$, $\mu = 0.1$, $\bar{\beta} = 0.0008$, $\bar{\gamma} = 0.25$, $\bar{k}_v = 0$, and $\bar{\rho} = 0.1$. Under these conditions, the system is overdamped in the open loop.

and avoid oscillations and significant variations (e.g., imagine what this response might imply for society).

(5) The control system must demonstrate *robustness* to nonlinearity; that is, the ability to maintain the system under control despite changes in operating conditions.

The Internal Model Control design procedure (Rivera et al., 1986; Morari and Zafiriou, 1989) is particularly well-suited to the controller design requirements previously noted, and can be applied to the linearized second-order model with zero shown in (16), augmented with a first-order filter with adjustable parameter λ_d. The design steps are summarized as follows:

Step 1: Obtain the IMC controller $\tilde{q}$. For this, the plant model must be factored into $\tilde{p}_+(s)$ and $\tilde{p}_-(s)$, corresponding to the non-minimum and minimum phase portions of the model respectively, as follows:

$$\tilde{p}(s) = \tilde{p}_+(s)\tilde{p}_-(s) \tag{17}$$

Considering that there is no delay or RHP zero in (16),

$$\tilde{p}_+(s) = 1 \tag{18}$$

the controller $\tilde{q}$ is then given by:

$$\tilde{q}(s) = \tilde{p}^{-1}(s) = \frac{s^2 + a_1 s + a_2}{b_1 s + b_2} \tag{19}$$

The controller $\tilde{q}$, although stable and causal, is improper.

Step 2: Augment (19) with a first-order filter $f(s)$ with adjustable parameter λ_d:

$$q = \tilde{p}^{-1}(s) f(s) \tag{20}$$

$$= \frac{s^2 + a_1 s + a_2}{(b_1 s + b_2)(\lambda_d s + 1)} \tag{21}$$

The result is a controller that is stable, causal, and semi-proper. Finally, it is necessary to obtain a classical feedback controller $c(s)$:

$$c(s) = \frac{q}{1 - \tilde{p} q} \tag{22}$$

$$= \frac{\frac{s^2+a_1 s+a_2}{(b_1 s+b_2)(\lambda_d s+1)}}{1 - \frac{1}{(\lambda_d s+1)}} \tag{23}$$

$$= \frac{s^2 + a_1 s + a_2}{(b_1 s + b_2)(\lambda_d s)} \tag{24}$$

It can be shown that $\frac{s^2+a_1 s+a_2}{(b_1 s+b_2)(\lambda_d s)}$ conforms to an ideal PID with filter structure:

$$c(s) = \left(\frac{s^2 + a_1 s + a_2}{\lambda_d\ s}\right)\frac{1}{(b_1 s + b_2)}$$
$$= \frac{a_1}{\lambda_d\ b_2}\left(1 + \frac{a_2}{a_1}\frac{1}{s} + \frac{1}{a_1}s\right)\left(\frac{1}{\frac{b_1}{b_2}s + 1}\right)$$
$$c(s) = K_c\left(1 + \frac{1}{\tau_I s} + \tau_D s\right)\left(\frac{1}{\tau_F s + 1}\right) \tag{25}$$

with tuning rules for this controller determined on the basis of the model coefficients in (16) and an adjustable parameter λ_d.

$$K_c = \frac{a_1}{\lambda_d\ b_2} \quad \tau_I = \frac{a_1}{a_2} \quad \tau_D = \frac{1}{a_1} \quad \tau_F = \frac{b_1}{b_2} \tag{26}$$

A further significant enhancement to the control strategy is to implement the IMC design as a two-degree-of-freedom (2DoF) classical feedback controller according to Figure 5. Such a controller will have individual adjustable parameters (e.g., λ_r, λ_d) to allow the user to independently adjust the speed of response for each degree-of-freedom (i.e., setpoint tracking versus disturbance rejection). The setpoint shaping prefilter resulting from a 2DoF design is

$$h(s) = \frac{\lambda_d s + 1}{\lambda_r s + 1} \tag{27}$$

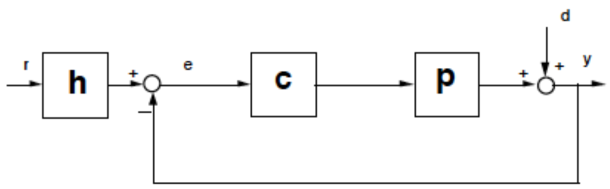

Fig. 5. Two-degree-of-freedom structure for classical feedback control. A setpoint shaping prefilter $h(s)$ allows for decoupling the setpoint tracking response from disturbance rejection.

4. SIMULATION CASE STUDIES

Many possible closed-loop control scenarios can be evaluated for this problem; in this paper, we describe two deterministic cases and one stochastic case. The first is one in which the control system performs badly. Consider the closed-loop responses to a setpoint change corresponding to a significant (90%) reduction in the initial endemic infected population (occurring at time $t = 5$) and a γ change of $+0.8$ (occurring at time $t = 40$ days), a k_v change of $+0.3$ (occurring at time $t = 80$ days), and a ρ change of $+0.25$ (occurring at time $t = 120$ days) for a single DoF controller ($\lambda_r = \lambda_d = 1$) and model parameters $B_r = 500$, $\mu = 0.1$, $\bar{\beta} = 0.0008$, $\bar{\gamma} = 0.25$, $\bar{k}_v = 0$ and $\bar{\rho} = 0.1$ as shown in Figure 6. This controller fails the desired specifications through offset in $I(t)$, resulting from $\beta(t) = 0$ (i.e., complete lockdown) during the first 40 days of the simulation, followed then by significant oscillations (in both $I(t)$ and $\beta(t)$. The controller rejects disturbance changes in γ, k_v, and ρ, but with underdamped behavior in $\beta(t)$. Any benefits from model-based tuning are lost as a result of improper settings for λ_r and λ_d.

Figure 7, in contrast, uses a 2DoF design with $\lambda_r = 5$ and $\lambda_d = 0.2$ that achieves an overdamped response in

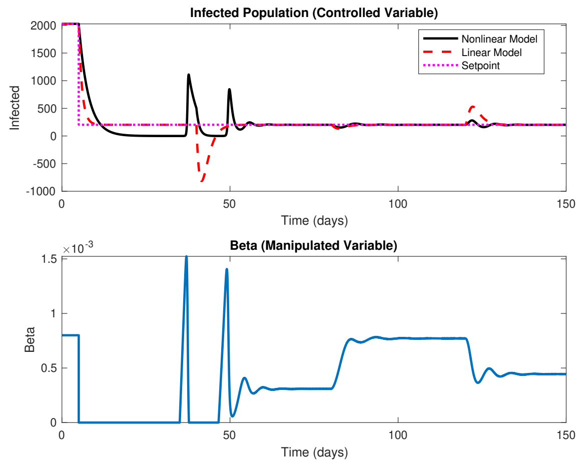

Fig. 6. Closed-loop response (for infected population, linear and nonlinear) to a setpoint change corresponding to a 90% reduction in the endemic infected population (occurring at time $t = 5$), a γ change of $+0.8$ (occurring at time $t = 40$ days), a k_v change of $+0.3$ (occurring at time $t = 80$ days), and a ρ change of $+0.25$ (occurring at time $t = 120$ days) for a single DoF IMC-PID with filter controller ($\lambda_r = \lambda_d = 1$) and model parameters $B_r = 500$, $\mu = 0.1$, $\bar{\beta} = 0.0008$, $\bar{\gamma} = 0.25$, $\bar{k}_v = 0$ and $\bar{\rho} = 0.1$.

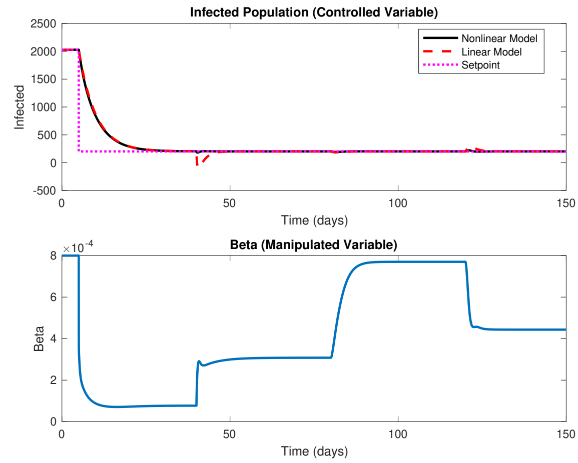

Fig. 7. Closed-loop responses (for infected population, linear and nonlinear) to a setpoint change corresponding to a 90% reduction in the endemic infected population (occurring at time $t = 5$), a γ change of $+0.8$ (occurring at time $t = 40$ days), a k_v change of $+0.3$ (occurring at time $t = 80$ days), and a ρ change of $+0.25$ (occurring at time $t = 120$ days) for a 2DoF IMC-PID with filter controller ($\lambda_r = 5, \lambda_d = 0.2$) and model parameters $B_r = 500$, $\mu = 0.1$, $\bar{\beta} = 0.0008$, $\bar{\gamma} = 0.25$, $\bar{k}_v = 0$ and $\bar{\rho} = 0.1$.

$I(t)$, avoids undershoot, and keeps β from ever reaching 0. In this case, controller response resulting from the γ change of $+0.8$ and k_v change of $+0.3$ (as before) leads to excellent setpoint tracking while allowing β to increase substantially, close to its initial value (implying a return to normalcy and pre-pandemic conditions). However, this implies the existence of more effective treatments (reducing

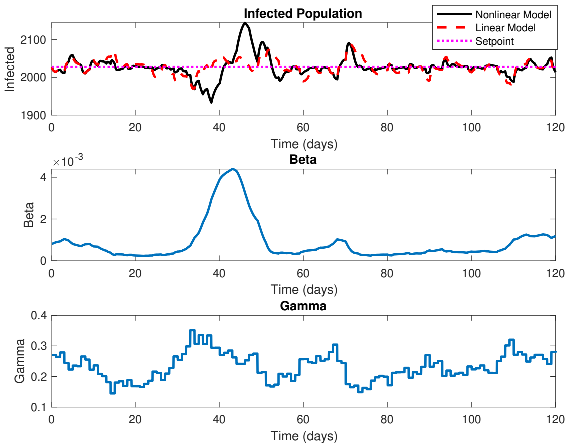

Fig. 8. Closed-loop responses (for infected population, linear and nonlinear) to a first-order autoregressive stochastic disturbance in $\gamma(t)$ ($\alpha = 0.85$), no setpoint change for a 2DoF IMC-PID with filter controller ($\lambda_r = 5, \lambda_d = 0.4$) and model parameters $B_r = 500$, $\mu = 0.1$, $\bar{\beta} = 0.0008$, $\bar{\gamma} = 0.25$, $\bar{k}_v = 0$ and $\bar{\rho} = 0.1$.

the duration of infectiousness) and a societal willingness for high rates of vaccination (30% of the susceptible population per day). Effective control is not just a product of sensible tuning, but also of "process design" considerations leading to these beneficial disturbance changes (in terms of increases in γ and k_v). If the virus mutates (resulting in increases in ρ), then the control system responds by reducing β, leading to more restrictive conditions that maintain the infected population at desired levels.

Fig. 8 shows the results of a stochastic simulation for the case of changes in $\gamma(t)$ (only) corresponding to a first-order autoregressive disturbance model with $\alpha = 0.85$. Increases in γ (which denote reduced infectiousness) are addressed by the controller with corresponding increases in $\beta(t)$. Nonlinearity effects are evident in the responses shown in Fig. 8; these can be mitigated through adjustments in λ_d.

5. SUMMARY AND CONCLUSIONS

The paper has presented an SIR epidemic model (featuring vaccination and loss of immunity) and shown that a natural feedback control system for this problem is obtained by applying IMC, leading to a 2DoF PID with filter controller. Its effectiveness has been shown in a demanding deterministic scenario involving a 90% reduction of the infected population under endemic conditions, as well as a stochastic scenario.

While this is clearly a very simplified evaluation of infectious disease control, the result is a simple and accessible computational model that could, in principle, be helpful to public health officials, and help inform the general public.

Many extensions of the work are possible. Enhancements to the SIR model through the inclusion of additional compartments have been proposed by many (Giordano et al., 2020); evaluating these would potentially be interesting. However, additional compartments would lead to higher-order systems and consequently(from applying IMC) to feedback control structures that would go beyond PID.

There is interest in applying both nonlinear IMC and MPC controller approaches to the problem. Dynamic theories of behavior change such as Social Cognitive Theory (Martín et al., 2020) can be incorporated into the model to address how $\beta(t)$ and $\gamma(t)$ are affected by behavioral constructs. We are furthermore interested in examining how Model Predictive Control (MPC) and data-driven frameworks such as "Model-on-Demand" MPC (Banerjee et al., 2024) could be used in this application.

ACKNOWLEDGMENT

Many thanks to Professor Cory Simon of the Department of Chemical, Biological, and Environmental Engineering at Oregon State University, whose excellent paper (Simon, 2020) seeded the ideas for the ChE 461 assignments that led to our initial results.

Support for this work has been provided by the National Science Foundation (US) through the Predictive Intelligence for Pandemic Preparedness (PIPP) program grant 2200161. The opinions expressed in this paper are the authors' own and do not necessarily reflect the views of the National Science Foundation.

REFERENCES

Banerjee, S., Khan, O., El Mistiri, M., Nandola, N., and Rivera, D. (2024). Data-Driven Control of Highly Interactive Systems using 3DoF Model-On-Demand MPC: Application to a MIMO CSTR (*in press*). *20th IFAC Symposium on System Identification (SYSID 2024)*.

Giordano, G., Blanchini, F., Bruno, R., Colaneri, P., Di Filippo, A., Di Matteo, A., and Colaneri, M. (2020). Modelling the COVID-19 epidemic and implementation of population-wide interventions in Italy. *Nature Medicine*, 26(6), 855–860.

Kermack, W.O. and McKendrick, A.G. (1927). A contribution to the mathematical theory of epidemics. *Proceedings of the Royal Society of London. Series A, Containing Papers of a Mathematical and Physical Character*, 115(772), 700–721.

Levenspiel, O. (1998). *Chemical Reaction Engineering*. John Wiley & Sons.

Martín, C.A., Rivera, D.E., Hekler, E.B., Riley, W.T., Buman, M.P., Adams, M.A., and Magann, A.B. (2020). Development of a control-oriented model of social cognitive theory for optimized mhealth behavioral interventions. *IEEE Transactions on Control Systems Technology*, 28(2), 331–346.

Morari, M. and Zafiriou, E. (1989). *Robust Process Control*. Prentice-Hall International.

Rivera, D.E., Morari, M., and Skogestad, S. (1986). Internal Model Control: PID controller design. *Industrial & Engineering Chemistry Process Design and Development*, 25(1), 252–265.

Rivera, D., El Mistiri, M., and Shi, Z. (2022). Using SIR epidemic modeling and control to teach process dynamics and control to chemical engineers. *IFAC-PapersOnLine*, 55(17), 380–385. 13th IFAC Symposium on Advances in Control Education ACE 2022.

Simon, C.M. (2020). The SIR dynamic model of infectious disease transmission and its analogy with chemical kinetics. *PeerJ Physical Chemistry*, 2, e14.